

Review

Anti-Coking and Anti-Sintering Ni/Al₂O₃ Catalysts in the Dry Reforming of Methane: Recent Progress and Prospects

Xingyuan Gao ^{1,2,†} , Zhiyong Ge ^{1,†}, Guofeng Zhu ¹, Ziyi Wang ¹, Jangam Ashok ³ and Sibudjing Kawi ^{3,*} 

¹ Department of Chemistry and Material Science, Guangdong University of Education, Guangzhou 510303, China; gaoxingyuan@gdei.edu.cn (X.G.); gezhiyong@gdei.edu.cn (Z.G.); zhugoufeng@gdei.edu.cn (G.Z.); wangzy@gdei.edu.cn (Z.W.)

² Engineering Technology Development Center of Advanced Materials and Energy Saving and Emission Reduction in Guangdong Colleges and Universities, Guangzhou 510303, China

³ Department of Chemical and Biomolecular Engineering, National University of Singapore, Singapore 117585, Singapore; chejang@nus.edu.sg

* Correspondence: chekawis@nus.edu.sg; Tel.: +65-6516-6312

† The authors contribute equally to this review.

Abstract: Coking and metal sintering are limitations of large-scale applications of Ni/Al₂O₃ catalysts in DRM reactions. In this review, several modification strategies to enhance the anti-deactivation property of Ni/Al₂O₃ are proposed and discussed with the recently developed catalyst systems, including structure and morphology control, surface acidity/basicity, interfacial engineering and oxygen defects. In addition, the structure–performance relationship and deactivation/anti-deactivation mechanisms are illustrated in depth, followed by prospects for future work.

Keywords: Ni; Al₂O₃; dry reforming of methane (DRM); anti-coking; anti-sintering



Citation: Gao, X.; Ge, Z.; Zhu, G.; Wang, Z.; Ashok, J.; Kawi, S. Anti-Coking and Anti-Sintering Ni/Al₂O₃ Catalysts in the Dry Reforming of Methane: Recent Progress and Prospects. *Catalysts* **2021**, *11*, 1003. <https://doi.org/10.3390/catal11081003>

Academic Editors: Andrzej Rogala, Jacek Gębicki and Izabela Wysocka

Received: 1 August 2021

Accepted: 17 August 2021

Published: 20 August 2021

Publisher's Note: MDPI stays neutral with regard to jurisdictional claims in published maps and institutional affiliations.

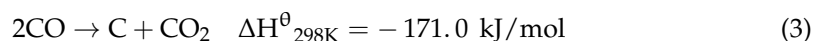
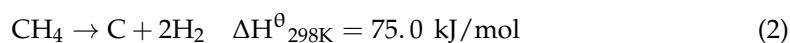


Copyright: © 2021 by the authors. Licensee MDPI, Basel, Switzerland. This article is an open access article distributed under the terms and conditions of the Creative Commons Attribution (CC BY) license (<https://creativecommons.org/licenses/by/4.0/>).

1. Introduction

In recent years, with the sustainable industrial development of human society and continuous growth of the population, the further exploitation of limited natural resources such as fossil fuels has attracted increasing attention [1]. The increasing energy consumption has led to the global greenhouse effect, which has caused great damage to the world environment and ecology [1,2]. Therefore, in order to protect the environment and save resources, it is urgent to explore technologies and methods that can replace energy and make better use of natural gas and other fossil fuel derivatives [3]. Methane (CH₄) and carbon dioxide (CO₂) are two main greenhouse gases. It is of great significance to realize their comprehensive transformation and utilization, in order to slow down the greenhouse effect [4]. In comparison with the partial oxidation of methane (POM) and steam reforming of methane (SRM), dry reforming of methane (DRM) is preferred because it can convert two greenhouse gases (CH₄ and CO₂) into syngas simultaneously; in addition, the DRM process is cheaper because it eliminates the complex gas separation of end products. Moreover, the ratio of H₂ to CO is close to 1:1, which is not only suitable for Fischer–Tropsch synthesis, but can also be used to produce high-value-added products such as methanol, acetic acid, dimethyl ether and oxyalcohol or long-chain hydrocarbons. Furthermore, syngas produced by DRM can be utilized for the storage of solar energy or nuclear energy, outperforming the other two reactions in terms of environmental and economic value [1–6].

The DRM reaction is a complicated process including several reactions:





The main reaction (Equation (1)) is a very energy consuming (endothermic) reaction, requiring a high temperature to activate the reactants. Catalysts can be added to reduce the activation energy (E_a) required for the reaction, saving the energy input and accelerating the reaction without being consumed [2,4,7,8]. Coke formation mainly originates from methane decomposition (reaction 2) and CO disproportionation (reaction 3). At a relatively high temperature, reaction 3 is probably inhibited thermodynamically; however, reaction 2 is promoted, thus leading to more carbon deposition. Meanwhile, reversed water–gas shift (RWGS) (reaction 4) affects the H_2 selectivity. On the other hand, considering the strong C–H chemical bond and highest oxidation state of C in CO_2 , the activation of CH_4 and CO_2 can be another challenge [9,10].

Noble metals (Rh, Ru, Pd, Pt, etc.) have features such as excellent performance and strong carbon deposition resistance in the DRM reaction [11,12]. For example, Ru-, Rh- and Pt-based catalysts possess a superior coke removal ability due to the high dispersion and small particle size [12]. However, limited by the high cost of precious metals, it is difficult to apply them on a large scale. In comparison, transition metals (Ni, Fe, Co, etc.) have drawn much interest because of their good catalytic performance and low cost. For example, Co has high affinity for the oxidative removal of carbon species [13]. In comparison, Ni is more reactive for CH_4 cracking and CO_2 activation [13]. Therefore, Ni-based catalysts have become promising for DRM reactions due to their rich reserves, low prices and high catalytic activity [14]. However, under high temperature and atmospheric pressure, carbon deposition and metal sintering lead to catalytic deactivation [14,15].

Strategies to improve the durability of Ni catalysts include enhancing the metal–support interaction (MSI) and generating reactive oxygen species. The former helps to inhibit metal sintering and greatly affects the catalytic performance of catalysts. The latter prevents or gasifies the carbon deposits. In addition, carbon deposition is closely related to the particle size of Ni. Due to the confinement effect of the support, the Ni particle size is reduced and the driving force of carbon diffusion in Ni crystals becomes weaker, significantly inhibiting the carbon deposition. Therefore, it is necessary to find a suitable support for Ni-based catalysts to enhance the metal dispersion, strengthen the MSI and introduce abundant oxygen defects [6]. Previous studies have shown that the coke formation can be reduced by adding metal oxides such as Al_2O_3 , SiO_2 , TiO_2 and ZrO_2 to enhance the MSI. Among them, alumina featured with its high specific surface area and appropriate pore size, exhibiting a stronger interaction with NiO and better catalytic performance compared with SiO_2 , TiO_2 and ZrO_2 [10]. Zhang et al. [10] prepared Ni-based catalysts with SiO_2 and Al_2O_3 as the supports. The results showed that less carbon deposition was formed on the Ni/ Al_2O_3 catalyst due to the stronger MSI between Ni and Al_2O_3 and the formation of smaller Ni particles. This was related to the formation of a NiAl_2O_4 spinel phase between the Ni precursor and Al_2O_3 during high-temperature calcination [16,17]. Moreover, oxygen vacancies can be generated in the reduced spinel structure, which promotes the adsorption and activation of CO_2 molecules to produce $\text{O}\cdot$ radicals to gasify the carbon deposits [17] (Table 1).

Despite the strong MSI and high surface area, the intrinsic acidity of Al_2O_3 activates the CH_4 decomposition but adversely affects the CO_2 adsorption, leading to a fast carbon deposition and a slow $\text{O}\cdot$ generation. The difference in reactant molecule activation rates results in coke formation and the coverage of Ni active sites [18]. In detail, the carbon nanotube formed in alumina firmly covers the Ni particles, causing the separation of the Ni active site from carbon dioxide and methane, and the weak interaction between Ni metal and Al_2O_3 by lifting Ni particles in the matrix, which subsequently leads to the migration of Ni particles to the outer surface of Al_2O_3 and easy agglomeration in the DRM reaction process [19]. To alleviate the above issue, Fahad S. Al-Mubaddel et al. [7,20] doped La_2O_3 into an acidic alumina support and found that the basic site density included a super basic site (related to monodentate carbonate) and low acid site density, which benefited the control of CH_4 dissociation and CO_2 chemisorption/dissociation on the catalyst surface

to oxidize the deposited carbon, greatly inhibiting the pulverization and graphitization of the carbon layer responsible for catalyst deactivation. However, another explanation was that on the acidic catalyst, methane is still activated on Ni, whereas carbon dioxide is dissociated on the catalyst support by forming carbonate/carboxylic acid.

Recently, strategies have been conducted to alleviate the carbon deposition and metal sintering of Ni/Al₂O₃ catalysts, including mesoporous alumina, morphology control, doping the second metal to form alloys, adding metal oxides to the support, reducing surface acidity, introducing oxygen defects and promoting surface oxygen mobility. However, reviews on related topics are still rare. Therefore, this paper will cover the latest research progress on the morphology and porosity control of alumina supports, surface acidity and alkalinity adjustments, alloy/MSI and oxygen defect formation, followed by the prospect of Ni/Al₂O₃ catalysts in DRM reactions in the future. It is believed that these strategies, proven effective in DRM reactions, will be promising in modifying the catalysts for other reactions such as steam reforming and tar reforming reactions, thus paving the way for a wide range of catalytic production techniques of syngas and clean energy.

2. Structure and Morphology Control

High-temperature thermal treatment in the DRM process will lead to the cracking of CH₄ and coke formation on the catalyst, and the sintering of metal particles, which covers the active sites and reduces the surface area, thus lowering the activity and stability of the catalyst. Therefore, an ideal support should enhance the metal dispersion and prevent carbon deposition [21]. Despite the admirable catalytic performance of Ni/Al₂O₃ catalysts in methane activation and CO₂ conversion, it also bears disadvantages such as coke deposition, sintering, phase transformation and reduction [21,22]. In 1992, a mesoporous material which can effectively control and reduce the metal deactivation rate was proposed for the first time, which is widely used in the field of catalysis [1]. Among them, mesoporous alumina, with a large surface area and ordered pore structures, anchors the metals within the structure and promotes metal dispersion, exhibiting better physicochemical properties than non-porous alumina in terms of the surface area, pore size and thermal stability [23,24]. Due to the low cost and excellent properties, mesoporous alumina has attracted the attention of researchers and is widely used as a catalyst support [25]. For example, Farshad Gholizadeh et al. [1] prepared cubic-ordered mesoporous alumina (COMA) as the support for Ni by adjusting the pH, which successfully dispersed Ni evenly into alumina support. The ordered mesoporous arrangement in COMA improved the confinement effect on the Ni⁰ active phase, i.e., it limited the well-dispersed Ni nanoparticles within the ordered mesoporous channels and imposed steric hindrance on Ni⁰ species [1]. On the other hand, the ordered mesoporous structure provided a large surface area for the dispersion of Ni nanoparticles, which enhanced the dispersion of Ni⁰ nanoparticles on the mesoporous support, thus strengthening the carbon deposition and sintering resistance of the catalyst [1,26]. The resulting conversion rates of methane and carbon dioxide were 93–99% and 91–97%, respectively, and the carbon deposition was only 5% in the 210 h stability test. In addition to the cubic mesoporous structure, a 2D hexagonal and mesoporous alumina exhibited similar effects on Ni particles. Karam Jabbour et al. [26] synthesized ordered and mesoporous Ni/Al₂O₃ through the “one-pot method”. In addition to the steric hindrance, Ni nanoparticles were highly dispersed in the Al₂O₃ support. After 13 h of testing, most nanoparticles were still anchored in the pores of the support, greatly reducing the possibility of sintering and producing almost no crystalline carbon.

The mesoporous structure of alumina not only promotes the DRM reaction activity by improving the dispersion of Ni nanoparticles, but also enhances the carbon resistance of the catalyst by strengthening the interaction between the metal and support. The mesoporous alumina-supported Ni catalyst prepared by Bian et al. [27,28] via a surface impregnation method benefited the formation of well-dispersed Ni nanoparticles (Table 1). Additionally, all Ni existed in the form of NiAl₂O₄ after calcination at 700 °C. Due to the strong MSI in NiAl₂O₄ spinel structure, Ni crystal size was only about 5 nm after reduction. Small

particle size was proven effective in inhibiting the carbon deposition, which was conducive to the DRM reaction. Meanwhile, the collapse of pores in mesoporous alumina generated larger pores without adverse effects on the pore volume, which significantly enhanced the coking resistance and stability of the Ni/Al₂O₃ catalyst. At 700 °C, the conversion of methane and carbon dioxide reached 77.6% and 85.4%, respectively, and the carbon deposition was as low as 3.8%. Compared with the mesoporous structure, hierarchical porous structures possess a multi-functional catalytic effect. Ma et al. [19] prepared an alumina support with both mesoporous channels and a macroporous structure. Benefiting from the bimodal pore distribution, large surface area and Ni dispersion were achieved; on the other hand, abundant channels were provided for the diffusion of reactants and product molecules. Due to the hierarchical structure, the prepared Ni/Al₂O₃ catalyst exhibited both a high conversion and strong resistance to carbon formation [19,29,30].

Mesoporous structure plays an important role in stabilizing the metal particles in Ni/Al₂O₃ catalysts by improving the MSI and confinement effect. Additionally, a large surface area and pore size alleviate coking and sintering during the DRM reaction. Similarly, the morphology of the alumina support can also reduce the size and increase the dispersion of Ni, thus improving the catalytic performance. For example, the alumina in the form of nanofibers promoted the dispersion of supported Ni metal particles, reduced their size, enlarged the Ni active surface area (96 m²/g), significantly inhibited the carbon deposition and sintering of Ni particles, increased the number of active sites, and facilitated the access of reactants into active nickel sites, positively influencing the stability and activity of Ni/Al₂O₃ catalyst [31,32]. In order to obtain better catalyst surface properties, ultrafine Ni particles and higher dispersion, Liang et al. [33] successfully synthesized raspberry-structured Al₂O₃ nanoparticles by the gas-phase method, which were well-mixed with the Ni precursor at acidic pH to form a precursor solution. Under evaporation-induced self-assembly (EISA), the stable Al₂O₃ nanoparticles gradually aggregated via capillary force to form ordered nanoparticle clusters (NPCs). The soluble Ni precursor was dried and deposited on the surface of Al₂O₃ NPCs. During thermal decomposition, the dried aerosol was transformed into nanostructures and NiO was formed in a single nanoparticle within the Al₂O₃ NPCs, followed by the transformation into Ni metal phase under H₂ thermal reduction. As shown in Figure 1a, ultrafine Ni crystals were homogeneously dispersed in Al₂O₃ NPCs. The Ni grain size was less than 7 nm and the metal surface area reached 129.9 m²/g, much better than the controlled Ni/Al₂O₃ catalyst. Due to the uniformly disperse nanoscale Ni catalyst and strong MSI with the raspberry-shaped Al₂O₃, the sintering of Ni grains was prevented and mossy carbon deposits were easily removed from the Ni surface. The resulting conversion of CH₄ and CO₂ were both enhanced by 20–40% at various reaction temperatures (T_{sur}), as shown in Figure 1b,c.

In addition to nanofibers and clusters, two-dimensional alumina nanosheets promote the dispersion of Ni nanoparticles and a reduction in nickel size because of their high BET specific surface area, leading to stronger anti-sintering and anti-coking properties, and a significantly improved stability. The initial methane conversion was 56.0%, which remained stable after 300 min of reaction. Similar trends were observed in CO₂ conversion and the H₂/CO ratio. The Ni nanoparticles were embedded into the alumina nanosheet, which triggered a strong MSI and enhanced the sintering resistance of the catalyst [34].

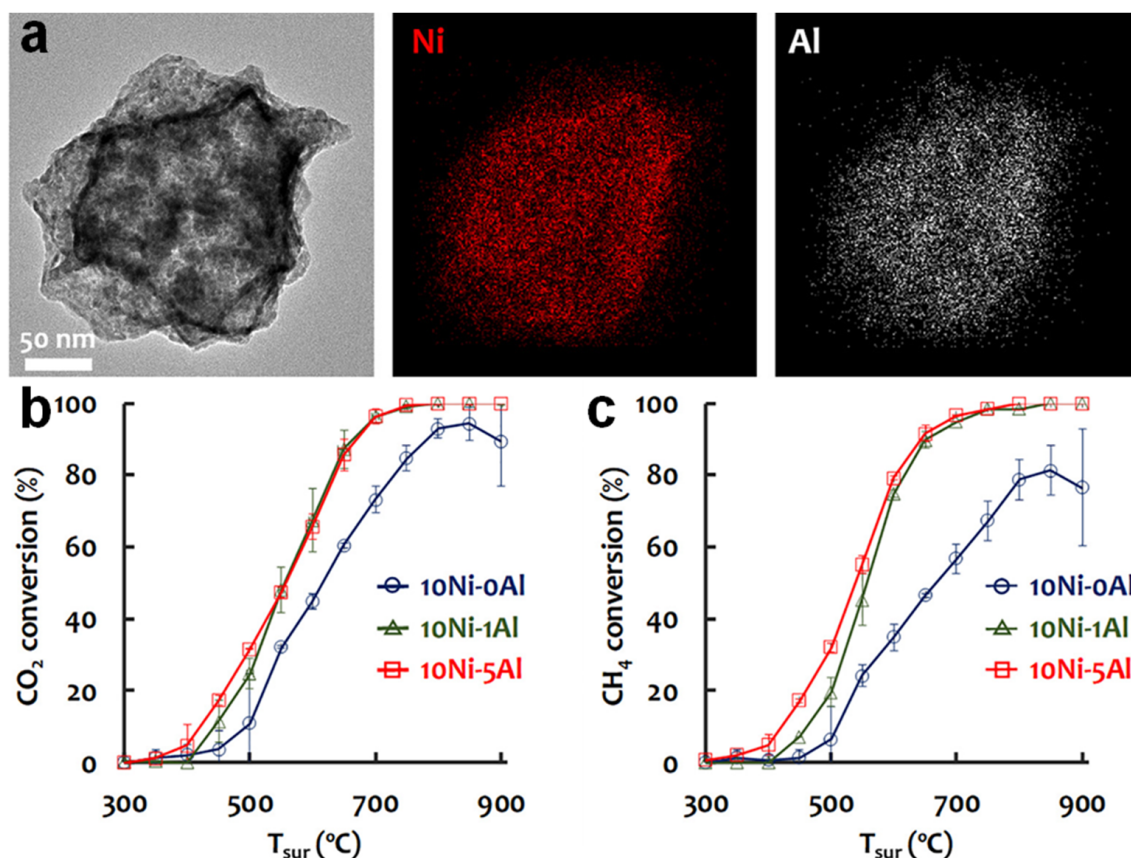


Figure 1. (a) HR-TEM image analysis of 10Ni-5Al with EDS elemental mapping. The scale bars are 50 nm. Activity tests of the catalysts using Ni-Al₂O₃ (b) X_{CO₂} vs. T_{sur}; (c) X_{CH₄} vs. T_{sur}. Reproduced with permission from [33]. Copyright 2020, Elsevier.

3. Surface Acidity/Basicity

In the DRM process, acidity and alkalinity are two of the key factors which determine the carbon on the catalyst surface. When Ni is supported on acidic alumina, the dissociation of methane is promoted so as to generate carbon deposition [28]. Increasing the basicity of the support through alkaline additives will enhance CO₂ chemisorption on the catalyst. On the one hand, enhanced basicity promotes the removal of coke formed in the process of CO disproportionation and methane cracking by oxidizing the carbon with CO₂, improving the stability of the catalyst. On the other hand, more basic sites facilitate the activation of CO₂ molecules, which is conducive to the catalytic conversion of reactants to syngas [35]. According to the methane reforming mechanism proposed by Tsipouriari et al. [36], the adsorbed CH_x intermediate on the support reacted with the -OH group to form the formic acid intermediate CH_xO, which subsequently decomposed into H₂ and CO. The highly alkaline metal oxide support can provide more -OH groups, which not only enhance the syngas yield from CH_xO decomposition, but also promote the adsorption and dissociation of CO₂, so as to produce more oxygen radicals near the catalytic active metal surface and inhibit the formation of carbon [37,38]. In addition, the surface acidity and alkalinity affect the electronic environment of the Ni active site to realize carbon inhibition, lowering the rate and degree of methane dissociation and CO disproportionation [39].

Basic oxides can be added to Al₂O₃ to reduce the acidity of Ni/Al₂O₃ catalysts. For example, La₂O₃ can cover the acidic sites of alumina and increase the basicity of the catalyst, which benefits the chemical adsorption and dissociation of CO₂, and prevents carbon deposition in DRM reaction. The balance between acidic and alkaline sites on the catalyst surface can control CH₄ decomposition, coke oxidation by CO₂, and the inhibition of the graphitization of carbon deposits [18,40,41]. On the other hand, La₂O₃ can adsorb CO₂ on alumina supports to form intermediate carbonate (La₂O₂CO₃), which is an active species

and further reacts with carbon on the surface near nickel to produce CO and La_2O_3 . This regeneration reaction of La_2O_3 reduces carbon deposition on the catalyst [42]. However, the generated $\text{La}_2\text{O}_2\text{CO}_3$ may lead to sintering and affect the stability of the catalyst.

Strong alkaline sites can enhance the CO_2 concentration on the catalyst surface, which not only increases the conversion rate of CO_2 , but also accelerates the gasification of surface carbon and delays the generation of inactive carbon [43,44]. In addition to La_2O_3 , MgO with a strong basicity can enhance the adsorption of CO_2 and its oxidation capability, thus reducing carbon deposition. Meanwhile, RWGS reactions could be inhibited, leading to a high H_2 selectivity. The Mg/Al ratio also determines the catalytic performance and deactivation behavior of Ni/ Al_2O_3 in the DRM reaction. When the ratio increased from 0.1 to 0.24, lower acidity and more defects in the MgAl_2O_4 spinel phase were obtained, achieving a 1/3 carbon deposition rate. However, with a further increase in the ratio to 0.5, despite the stronger basicity, the loss of mesopores and lower surface area adversely affected the activity [45]. Therefore, if the support alkalinity is too strong, carbon deposition may not be inhibited, leading to an unstable conversion. Apart from adjusting the Mg/Al ratio, the addition of Y_2O_3 introduces more weak and medium alkaline sites into the Ni/ Al_2O_3 catalyst (Table 1). Moreover, 1.5 wt.% Y_2O_3 optimized the surface basicity, exhibiting high and stable conversions of CH_4 (78.3%) and CO_2 (73.9%) [46,47].

In addition to metal oxides, P as a non-metal element can enhance the coke resistance and stability of Ni/ Al_2O_3 in the DRM reaction by adjusting the acidity. The 2 wt.% P-modified Ni/ Al_2O_3 catalyst displayed the lowest acidity and exhibited excellent anti-coking property in 100 h of reaction. When the basicity of the catalyst was increased, acidic carbon dioxide molecules were more likely to adsorb on the catalyst surface; therefore, the Boudouard reaction was promoted, which gasified the deposited carbon. Meanwhile, with the increase in P content, the generated AlPO_4 interfered with the interaction between the active Ni and Al_2O_3 , so as to improve the reducibility of NiO to produce more active sites [48].

As well as the addition of basic oxides, the pretreatment atmosphere can affect the surface acidity and basicity. Compared with air calcination, Ar pretreatment could enhance the basic sites together with the addition of ethylene diamine tetra-acetic acid (EDTA) due to the promotional effect of carbon residues at the interface of Ni^0 and La_2O_3 [49]. In another case, N_2 calcination would increase the amount of Lewis acid sites on Al_2O_3 , which strongly interacted with metallic Ni and reduced the Ni electron density, thus inhibiting metal sintering and carbon deposition [39,50–52].

Generally speaking, as an acidic support, Al_2O_3 induces methane cracking and slows down the activation of CO_2 , thus resulting in carbon deposition. The acidity and basicity of the catalyst can be adjusted by adding alkaline metal oxides such as La_2O_3 and MgO or non-metal P and modifying the synthesis method, such as the pretreatment atmosphere, to promote the gasification of coke. However, excessive alkalinity will also lead to carbon deposition. Therefore, the basicity of the catalyst should be optimized to balance the activity and stability of Ni/ Al_2O_3 in the DRM reaction.

4. Interfacial Engineering

By tuning the spatial and electronic environment via Ni alloy formation and adjusting the interaction between Ni and Al_2O_3 with the addition of another support, the metal agglomeration and coking process can be inhibited; additionally, the activation of CH_4 and CO_2 could be enhanced, thus leading to a good activity and stability in DRM reaction.

4.1. Alloy Formation

Ni-based catalysts will be deactivated due to the loss of active sites when sintering and carbon deposition occur in DRM reactions. By forming alloys with other metals such as noble metals (Pt, Rh, Ru) and transition metals (Fe, Co), the catalyst will possess a stable structure, enhanced reducibility and large specific surface area, resulting in a better performance than that of a single Ni catalyst. Additionally, alloy formation can lead to a

smaller metal particle size, which is conducive to the inhibition of carbon deposition and the gasification of carbon. For example, Ni and Co can form alloys to promote oxygen adsorption, prevent the adsorption of carbon, limit RWGS reactions and inhibit the sintering of Ni. As for Cu–Ni and Mg–Ni alloys, more active sites are generated on the surface along with the reduction in particle size and better dispersion [2,5,53]. The following sections will introduce the effect of Ni alloys with different metals on the catalytic performance of Ni/Al₂O₃ in DRM reactions.

4.1.1. Noble Metal–Ni Alloy

In DRM reactions, the selection of active metals plays an important role in inhibiting coking and enhancing the catalytic performance. Noble metals are widely used in reforming reactions and show better carbon deposition resistance than Ni in DRM reactions. Therefore, noble metals have been introduced into Ni/Al₂O₃ catalysts, forming a beneficial synergy. In addition, the bimetallic catalyst can promote the activation of C–H bonds in methane and maintain the constant conversion of methane at high temperatures.

It is well known that Ni²⁺ ions are not active in methane reforming, and their coverage on the metal Ni surface reduces the active sites, resulting in a poor activation of methane [54]. Adding a small amount of Pt to Ni can inhibit the oxidation of Ni. This is because Pt cannot be oxidized below 300 °C, which stabilizes the Ni and prevents it from being oxidized. The addition of Pt also significantly lowers the reduction temperature because H₂ molecules overflow on the surface of Pt; after adsorption and dissociation, the generated H atoms react with NiO to form Ni metals. In addition, the interaction between Pt and Ni sites in the closed region and the dilution effect of Pt lead to a higher dispersion of Ni metal nanoparticles with a smaller size, resulting in a weak interaction with the tetrahedral structure of CH_x species, which slows down the complete decomposition of CH₄ into coke [55]. At the same time, the Ni–Pt alloy promotes the formation of surface hydroxyl groups and improves the rate of carbon gasification [56,57]. Figure 2a shows that the optimal Pt loading was 0.4 monolayer, which exhibited the highest methane conversion due to the small alloy size. Meanwhile, it also presented an excellent sintering resistance (nearly no size change during the reaction). However, when the proportions of Pt continued to increase, larger particles were formed, resulting in higher activation energy (96.4 vs. 86.2 kJ/mol) and a poor activity (Figure 2a). On the other hand, when the calcination temperature was above 600 °C, separation of the Ni–Pt alloy occurred to produce large Pt ensembles (Figure 2b), which excessively promoted the decomposition of methane into surface carbon and intensified the deactivation rate of the catalyst [53].

In addition to the Ni–Pt bimetallic catalyst, the alloy formed by Rh and Ni presents high stability and strong anti-coking ability, which exerts a positive effect in DRM reactions [58–60]. Compared with Ni/Al₂O₃ catalysts, the interaction between Ni and Rh improves the conversions and H₂ yield with less coking and improved stability. This enhanced performance is due to the reduction in NiO species by high concentrations of spilled H₂ and the inhibition of CO disproportionation and CO₂ hydrogenation reaction [61]. Damyanova et al. [62] showed that the strong interaction between Rh and Ni not only improved the reducibility of NiO, but also increased the surface distribution of Ni, producing a small and uniform Ni particle (5 nm in diameter) evenly distributed on the Al₂O₃ support. In addition to the reducibility and particle size, the surface charge of the nanoparticles may also determine the activity. Due to the low surface energy of Rh relative to Ni, Rh atoms were preferably on the top of Ni layer. According to the Pauling scale, it could be inferred that negatively charged Rh and positively charged Ni coexisted in the Ni–Rh alloy due to the different electronegativities. During the reaction, Ni⁰/Niⁿ⁺ and/or Rh⁰/Rhⁿ⁺ pairs may act as catalytic active sites, which probably enhanced the conversion of methane and the H₂ yield of Rh–Ni/Al₂O₃. Due to the above merits, the conversion of methane and carbon dioxide at 650 °C reached about 80% and 90%, respectively, with a high H₂ selectivity (H₂/CO ratio = 1.79). Over a 3 h reaction test, no conversion drop

was shown for Rh–Ni/Al₂O₃, but a decrease in activity of over 10% was presented for Ni/Al₂O₃ [62].

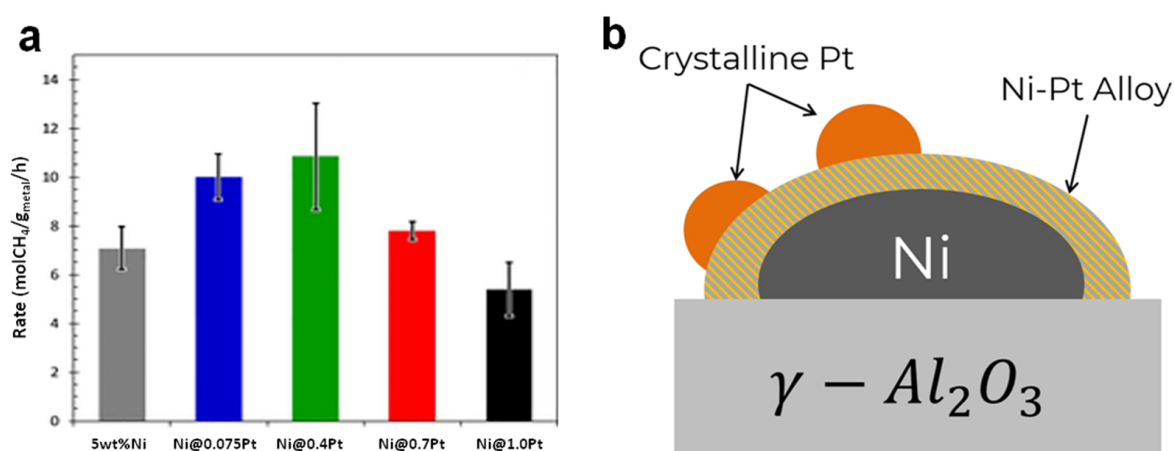


Figure 2. (a) Steady state CH₄ conversion rates at 550 °C. (b) Proposed structure for electroless deposition-derived Ni–Pt samples. Reproduced with permission from [53]. Copyright 2020, Elsevier.

In summary, for Ni/Al₂O₃ catalysts, due to the presence of oxygen, the surfaces of Ni particles are easily oxidized and covered with a layer of Ni²⁺ ions, reducing the methane reforming activity. In contrast, the addition of noble metals into Ni/Al₂O₃ catalysts exhibits better catalytic performance due to the reducibility and intrinsic high activity of noble metals. In addition, noble metals and Ni exist in alloy states with a strong interaction, which effectively inhibits the agglomeration of nickel. Moreover, the generation of surface hydroxyl groups is beneficial for the removal of carbon deposition, so as to maintain the high activity and stability in DRM reactions.

4.1.2. Transition Metal–Ni Alloy

Although noble metals are good candidates for the formation of Ni alloys, the cost and scarcity limit their large-scale applications. In contrast, due to the satisfactory activity and low cost, transition metals have drawn much interest as dopants in Ni/Al₂O₃ catalysts in DRM reactions. Representative metals such as Cu, Fe and Co possess similar electronic structures and chemical properties to nickel, which facilitates their incorporation to form nickel-based alloys with synergistic effects, such as high dispersion, good activity and reduced coking tendency [63–65].

Among the transition metals, due to the similar lattice structure between CuO and NiO, the formation of a uniform NiO–CuO solid solution is promoted during calcination; after subsequent reduction in H₂, Cu can form alloys with Ni in Ni–Cu/Al₂O₃, which, in turn, stabilizes Ni and prevents the generation of large crystals. The Ni–Cu alloy shows excellent activities and effectively reduces the coking and metal sintering in DRM reactions. For example, Chatla et al. [66] doped Cu to Ni/Al₂O₃; the overlapping spatial distribution of Ni and Cu suggested the complete incorporation of copper into nickel lattices to generate Ni–Cu alloy particles, which directly tuned the electronic properties of the active metal sites. Additionally, the Ni–Cu alloy facilitated the H₂ spillover and effectively inhibited the formation of a NiAl₂O₄ spinel (lower temperature shift for the reduction temperature), improving the reducibility of metal and increasing the number of active sites (Figure 3a) [67]. Moreover, the average particle size of Ni–Cu alloy (4 nm) was smaller than that of single Ni catalyst (9 nm), indicating a higher dispersion of metal phase with the addition of Cu. Apart from the enhanced dispersion and reducibility, the higher activation barrier of dehydrogenation of CH₄ on medium content Cu catalysts suggested a less possibility of carbon formation. In addition, the carbon adsorption energy of single Ni catalyst was higher than that of Ni–Cu alloy, which indicated a lower surface

coking tendency of Ni–Cu/Al₂O₃. Moreover, with the Cu doping, the carbon elimination barrier was reduced, thus enhancing the ability of carbon gasification to carbon monoxide. Due to the promotional effects of medium Cu content in Ni–Cu/Al₂O₃, both the initial conversion of CH₄ and stability were enhanced (Figure 3b). Additionally, coke formation was effectively alleviated and most carbon formed was amorphous instead of graphitic, which was more easily gasified (Figure 3c). However, when the content of Cu was too high, the activation barrier of methane dehydrogenation would be greatly increased, hindering the process of the DRM reaction. Additionally, the Ni active site could be covered and was more prone to sintering [67]. Therefore, Cu content is crucial because it is related to the surface arrangement of Ni and Cu atoms. On one hand, the Cu content must be high enough to allow alloying with Ni; on the other hand, excessive Cu may cause segregation on the catalyst surface and the formation of Cu clusters, which will lead to the interruption of DRM reactions [68].

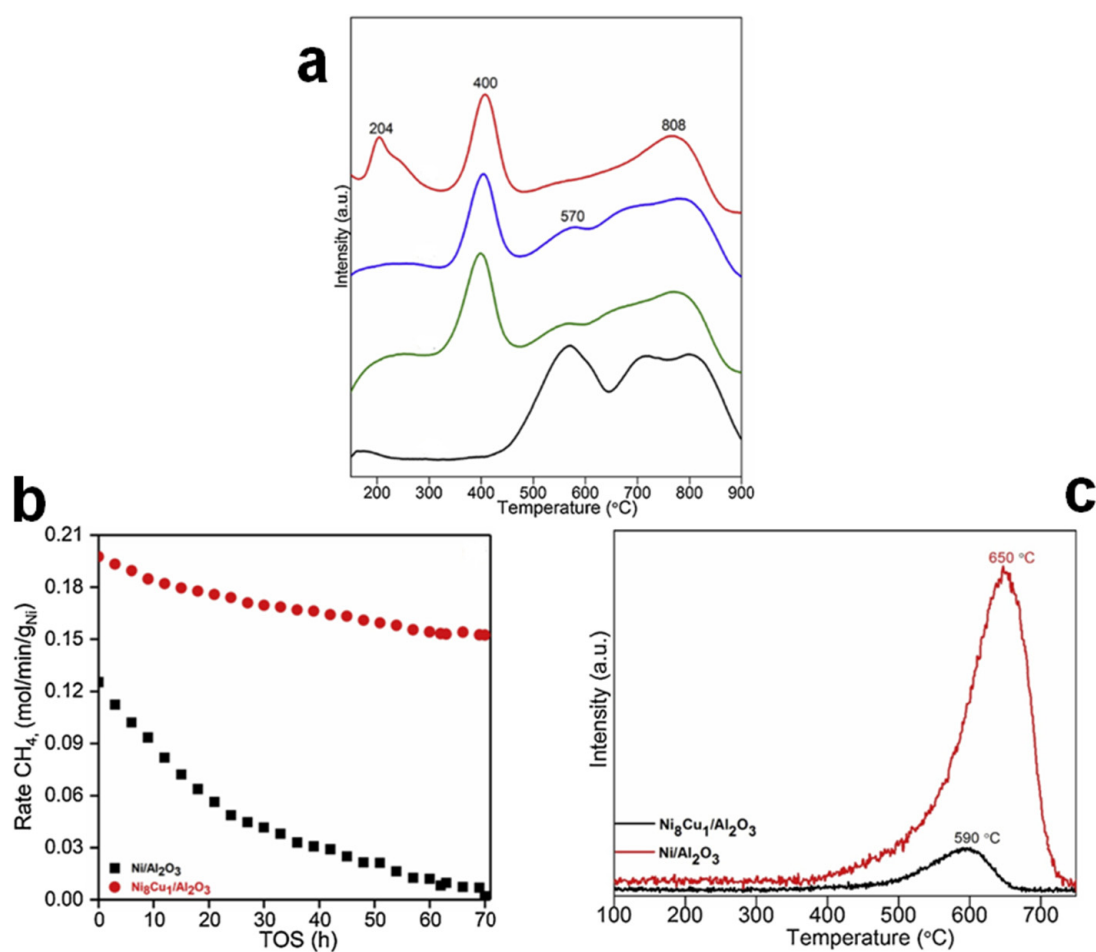


Figure 3. (a) H₂-TPR analysis of fresh calcined Ni/γ-Al₂O₃ (black), Ni₁₀Cu₁/γ-Al₂O₃ (green), Ni₈Cu₁/γ-Al₂O₃ (blue) and Ni₃Cu₁/γ-Al₂O₃ (red) samples. (b) CH₄ conversions rates vs. TOS for the CO₂ reforming of methane at 650 °C. (c) O₂-TPO profile of spent catalysts after DRM performance at 650 °C for 70 h TOS. Reproduced with permission from [66]. Copyright 2020, Elsevier.

Although Ni–Cu shows excellent ability in reducing carbon deposition, Ni–Co catalysts present higher metal dispersion than Ni–Cu. By comparing the promotion effects of Cu and Co on Ni/Al₂O₃ catalyst, the Ni–Cu active sites are unevenly dispersed due to the sintering of copper particles in the calcination stage. On the contrary, uniform morphology, high surface area, large pore size and porosity, and well-dispersed particles can be achieved in Ni–Co/Al₂O₃ nano catalyst [22,65,69]. These metal particles are con-

fined in the porous structure of alumina matrix, which helps to resist particle aggregation, in turn improving the resistance to carbon deposition [22]. Liu et al. [63] synthesized a Ni–Co/ γ -Al₂O₃ bimetallic catalyst; the addition of Co increased the metal dispersion by 12 times. In addition, the higher reduction temperature in TPR profiles of Ni–Co/Al₂O₃ (Figure 4a) suggested a stronger MSI, which anchored the active metal particles in the cavities, enhancing the sintering-resistance and forming a homogeneous size distribution, thus improving the activity and stability in DRM reactions [13,22,65]. On the other hand, the existence of Co led to the formation of new active sites and the enhancement of the alkalinity of bimetallic catalysts, as shown in the higher peak intensity in Figure 4b, which benefited the adsorption CO₂ molecules and accelerated the oxidation of surface carbon species. Benefiting from the above properties, as shown in Figure 4c,d, the catalytic activities of the Ni–Co alloy catalyst were higher than those of the single metal counterparts, and the conversion rates did not drop obviously after testing at 700 °C for 3 h, which could be attributed to the high metal dispersion, a large number of active sites, abundant basic sites and strong MSI. In order to further clarify the synergistic effect of Ni–Co alloy, Aghaali et al. [22] prepared a well-dispersed Ni–Co alloy on an Al₂O₃ support (Table 1). Co possessed a high affinity for carbon species and promoted the removal of carbon by oxidation; Ni was more active for methane cracking. The strong Ni–Co bimetallic interaction not only promoted the Boudouard reaction and the oxidation of adsorbed CH_x species, but also enhanced the H₂ yield. The resulting carbon deposition was only 1.3 wt.%, which could be easily removed by oxidation.

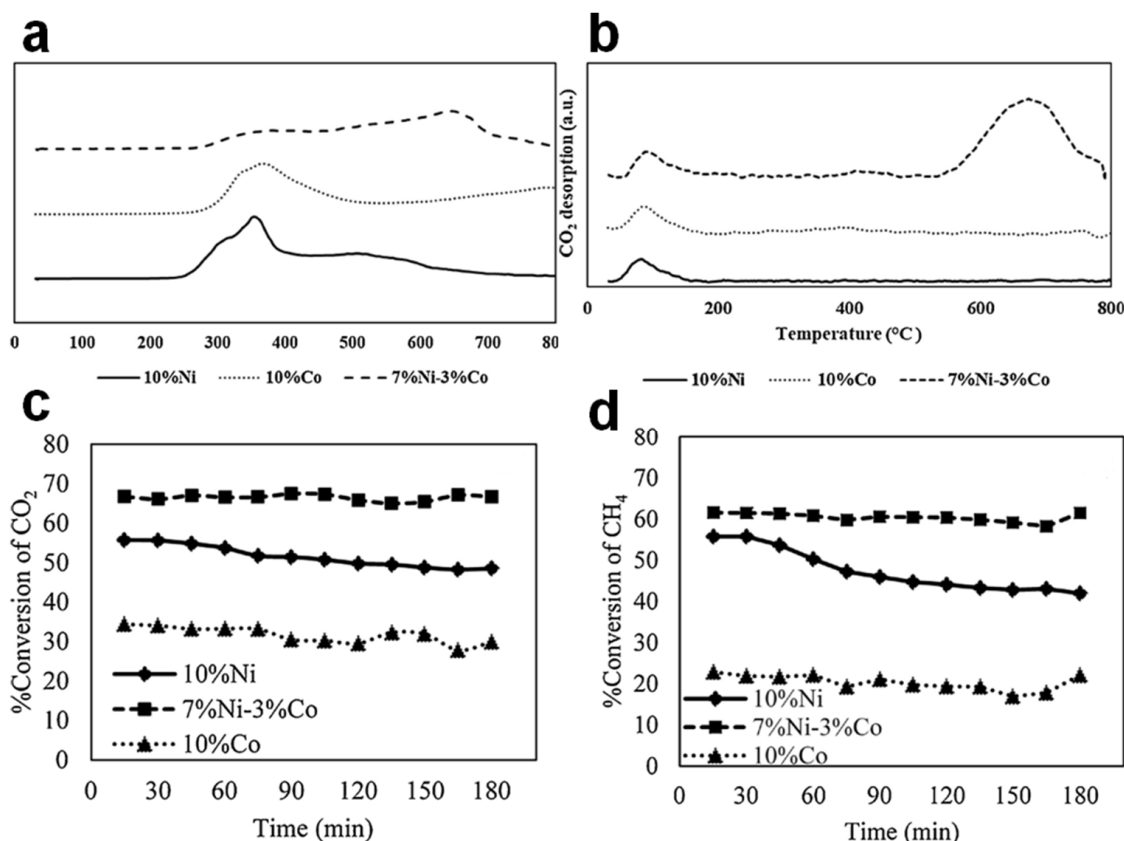


Figure 4. (a) The TPR profiles of the nickel–cobalt monometallic and bi-metallic catalysts over γ -Al₂O₃-HY zeolite. (b) CO₂-TPD profiles of the nickel–cobalt monometallic and bi-metallic catalysts over γ -Al₂O₃-HY zeolite. Catalytic performance of (c) CO₂ conversions and (d) CH₄ conversions. Reproduced with permission from [63]. Copyright 2020, Elsevier.

In addition to Cu and Co, Fe is active and is widely used in alloy catalysts because of its good redox ability [70]. Ray et al. [71] found that Fe and Ni formed FeNi₃ alloys whose H₂ chemisorption concentration was greater than that of Ni–Co/Al₂O₃. Despite the

higher activities of Ni–Co/Al₂O₃, Ni–Fe/Al₂O₃ exhibited a lower deactivation rate and better stability. Meanwhile, the carbon deposition rate was slower in Ni–Fe/Al₂O₃ than that in Ni–Co/Al₂O₃ [71]. Therefore, Ni–Fe/Al₂O₃ could be a promising DRM catalyst. Fe and Ni have similar electronic structure and chemical properties; therefore, it is easy for Fe and Ni to react with each other to form a bimetallic Ni–Fe alloy after reduction. The synergistic effect can reduce the sintering and carbon deposition in DRM reactions. Li et al. [72] synthesized a Ni–Fe alloy supported on ordered mesoporous alumina through the “one pot” evaporation-induced self-assembly (EISA) method (Table 1). The metal sites were confined in the alumina pores, which minimized the metal migration and sintering. Due to the strong redox properties of Fe, the oxygen storage capacity of the catalyst was enhanced so as to remove carbon deposition. To further elucidate the anti-coking mechanism, Kim et al. [70] synthesized a Ni–Fe/Mg_xAl_yO_z catalyst, in which iron migrated onto the surface of the support by FeO/Fe redox cycle. During the reaction, Fe was partially oxidized to FeO, resulting in partial de-alloying and the formation of a Ni-rich Ni–Fe alloy. The generated FeO was located on the surface of the catalyst and covered a small part of Ni-rich particles. The intimate contact of FeO and nearby Ni–Fe facilitated the coke oxidation and reduction of FeO into the Ni–Fe alloy through a redox mechanism, which significantly inhibited the carbon deposition and improved the stability of the Ni–Fe/Al₂O₃ catalyst.

4.1.3. Ni–Sn Alloy

In addition to noble metals and transition metals, other main-group metals such as Sn exhibit good catalytic activities in DRM. The addition of a small amount of Sn to Ni/Al₂O₃ can obtain a bimetallic catalyst with a higher activity, reduced carbon deposition and improved stability compared with a single Ni catalyst. Da Silva et al. [73] found that due to the interaction between Ni and Sn, this bimetallic catalyst was excellent in the activity, stability and selectivity of syngas production (Table 1). Regarding carbon deposition, the Ni–Sn alloy could promote the oxidation of carbon on the catalyst surface. With a similar electronic structure to carbon, interactions between the Sn 5p orbital and Ni 3d electrons were strengthened. The change in electronic structure affected the reactant adsorption and hindered carbon nucleation on the active Ni sites, thus reducing the possibility of nickel carbide formation as the coke precursor and avoiding the diffusion of carbon to form large coke aggregates. After the DRM reaction, the surface of the Ni/Al₂O₃ catalyst was covered by graphitized carbon, whereas for Ni–Sn/Al₂O₃, only part of the catalyst surface was covered by filamentous carbon, which was softer and easier to remove, doing little harm to the deactivation of the catalyst. Therefore, the bimetallic catalyst still exposed most of the active sites after continuous operation, enhancing the stability for DRM reactions [74,75]. In addition to the anti-coking performance, the addition of Sn improved the anti-sintering ability, increased the metal active sites, and enhanced the yield of syngas, especially H₂ yield. Due to the gasification of residual carbon during the reaction, the volume originally occupied by carbon became pores, where uniform Ni–Sn alloy particles were highly dispersed, which could reduce the metal sintering. In addition, the affinity between H and Ni became weak due to the existence of Sn, suggesting an easier desorption of H₂ from the surface of the alloy, which inhibited the side reactions such as RWGS, resulting in fewer by-products and higher H₂ yield. On the other hand, Sn promoted the oxidation of reaction intermediates such as CHO, benefiting the formation of the final product—syngas [74]. However, the activity of the catalyst was affected by the content of Sn. A lower loading of Sn enabled an improved activity and reduced the carbon deposition. If excessive Sn was doped, the increased electron density originating from the hybridization of the Ni 3d orbital and Sn 5p orbital greatly hindered the activation of CH₄, thus leading to a low catalytic activity in DRM reactions [73].

4.2. Metal–Support Interaction (MSI)

A metal–support interaction (MSI) helps to anchor nickel particles on the support to inhibit their sintering, modifying the metal size, dispersion, surface area and reducibility of the nickel catalyst, thus enhancing the activity and stability of the DRM reaction [76,77]. For example, the unique stability of the Ni/Ce–Al₂O₃ catalyst was attributed to the good morphology and sufficient MSI, which stabilized the nickel species on the Al₂O₃ support and inhibited coking by promoting the Boudouard reaction [78]. In addition, the introduction of La prevented the sintering of Ni under harsh reaction conditions by enhancing the interaction between Ni metal and the Al₂O₃ support, leading to improved activity and stability [18]. However, a high temperature is needed to reduce the metals strongly interacting with the support, which may cause metal sintering under an intensified thermal treatment and the loss of active surface area for the adsorption and activation of reactant molecules in the DRM reaction. Thus, an optimized MSI will be appropriate considering the reducibility and stability of metal sites on the support.

Ni can easily react with Al₂O₃ to form a NiAl₂O₄ spinel at a temperature above 600 °C. The formation of this aluminate enhances the MSI and shows good anti-sintering and anti-coking properties in the DRM process. In terms of size control, the Ni size reduced from NiAl₂O₄ was 11 nm smaller than that derived from naked Al₂O₃, suggesting that the presence of NiAl₂O₄ stabilized the Ni particles at a high temperature. In addition, the incomplete reduction of NiAl₂O₄ produced a Ni_xAl_yO_z support, which was considered a defective NiO–Al₂O₃ solid solution species with multiple Ni²⁺ defects, also stabilizing the size of Ni. In terms of carbon deposition, the coke formed on Ni/Al₂O₃ produced by NiAl₂O₄ was only 8 wt.%, much lower than that on the Ni reduced from NiO in Ni/Al₂O₃ (37 wt.%) after 100 h of DRM. This difference in coke resistance could be explained by the fact that the easily reducible NiO species produced Ni sites with weak MSI; on the contrary, the partial reduction and extraction of Ni²⁺ ions in NiAl₂O₄ were expected to possess sufficient interaction with Al₂O₃ to inhibit carbon deposition. In addition, in a reductive atmosphere, NiAl₂O₄ formed a defective Ni_xAl_yO_z phase, which was likely to exhibit high surface oxygen mobility. Therefore, the high stability of NiAl₂O₄ could also be related to the high carbon gasification rate [76]. However, the NiAl₂O₄ spinel needs a high temperature to be reduced to NiO and Ni due to strong MSIs. Thus, the amount of active Ni may be limited, and high-temperature metal sintering can occur. Therefore, the formation of a NiAl₂O₄ spinel may lead to the deactivation of the Ni/Al₂O₃ catalyst in the methane reforming reaction [79,80]. In order to reduce the formation of NiAl₂O₄ and alleviate the excessive MSI, other metal oxides can be added to reduce the interaction between Ni and Al₂O₃. For example, when calcium was added to Al₂O₃, calcium competed with nickel to interact with alumina and tended to form calcium aluminate, reducing the possibility of the subsequent formation of nickel aluminate and producing more reducible Ni species, as shown in the lower temperature shift of the reduction peak in TPR profiles (Figure 5a). Meanwhile, Ca could increase CO₂ adsorption and activation, increase methane conversion and reduce carbon deposition. However, a further increase in calcium content would decrease the specific surface area and increase the electron density on the surface of nickel, which reduces the adsorption of methane molecules and decreases the conversion (Figure 5b) [81].

In addition to Ca, rare earth metals can also adjust the MSI. The presence of Ce helps to increase the dispersion of metal nickel with a strong MSI, inhibiting the growth of carbon whiskers and metal sintering, and generating a smaller Ni particle size [82]. Unlike ceria, which tends to exist in the form of crystals on the catalyst surface, La₂O₃ presents a monolayer dispersion, possessing a strong interaction between La₂O₃ and alumina. Additionally, the introduction of La prevents the sintering of Ni under harsh reaction conditions by enhancing the interaction between Ni metal and support. However, the monolayer La₂O₃ will cover the Ni active sites, resulting in reductions in the active specific surface area. Li et al. [18] doped La into Ni/Al₂O₃ via a novel synthesis method. By calcining La₂O₃ on Al₂O₃ in a CO₂ atmosphere, La₂O₂CO₃ was generated to replace La₂O₃,

so as to prevent Ni from entering the bulk phase of Al_2O_3 to form the spinel phase, improve the reduction degree of nickel and increase the specific surface area. Compared with blank Ni/ Al_2O_3 , La-modified Ni/ Al_2O_3 showed higher activities in the DRM reaction (Table 1).

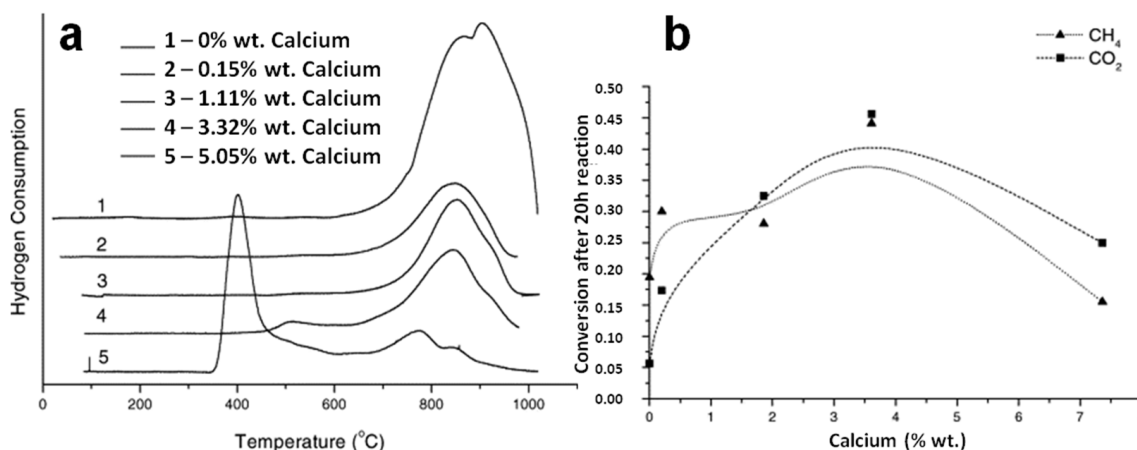


Figure 5. (a) Temperature-programmed reduction profiles of samples with addition order 1Ca2Ni. (b) Change in total methane and carbon dioxide conversion after 20 h reaction with amount of calcium of 1Ni2Ca. Reproduced with permission from [81]. Copyright 2003, Elsevier.

5. Oxygen Defects and Surface Oxygen Species

It is well known that lattice/surface oxygen and oxygen vacancy enhance the mobility and adsorption of oxygen and effectively remove carbon deposition in the DRM reaction [83]. Due to the high reducibility, facilitated oxygen mobility and the redox cycle of $\text{Ce}^{4+}/\text{Ce}^{3+}$, CeO_2 is reversibly converted to non-stoichiometric oxides, thus providing high oxygen storage capacity and oxygen mobility [84–87]. The redox pair is formed due to the electronic interaction between CeO_2 and Ni. Ce is rich in d-orbital electrons whereas Ni has unfilled d-orbitals; thus, the unfilled d-orbital of Ni atom can accept the d-electrons of Ce. Under a reducing atmosphere, CeO_2 can be converted to the mixture of Ce_2O_3 and CeO_2 . The catalytic mechanism of this redox pair on the DRM reaction is as follows: the reactant CO_2 first adsorbs on the basic sites, followed by dissociation on Ce_2O_3 to produce CO and CeO_2 through the transfer of electrons. Then, CeO_2 reacts with the deposited carbon produced by CH_4 dehydrogenation, transforming back into Ce_2O_3 again. Meanwhile, due to the dissociation of CO_2 , the adsorbed oxygen atoms and other oxygen-containing species are responsible for inhibiting the formation of carbon. Therefore, the presence of CeO_2 and Ce_2O_3 in the catalyst will improve the inhibition of surface carbon formation [86,88]. In another explanation, ceria can enhance the reversible oxygen adsorption/release capacity of Ni/ Al_2O_3 catalysts. With the flow of surface oxygen species, CO_2 molecules are adsorbed to form bidentate carbonate, which react with surface carbon species, resulting in a higher CO_2 conversion and lower carbon formation [35,86].

Based on the above mechanism, Chen et al. [89] prepared a series of Al_2O_3 -supported Ni catalysts modified with different amounts of CeO_2 by incipient wet impregnation (Table 1). As shown in Figure 6a, under operating conditions, Ce existed as a mixture of Ce^{3+} in CeAlO_3 and Ce^{4+} in CeO_2 . Due to the lower oxidation state and abundant oxygen vacancies, CeAlO_3 adsorbed and dissociated CO_2 to generate CO and active oxygen species, which formed an oxidative environment around nickel sites, resulting in the gasification of carbon atoms at the nickel–support interface immediately before the nucleation and growth of the graphene layer, greatly improving the carbon resistance of the catalyst. Subsequently, the previously generated CeO_2 reacted with CO_2 to produce carbonate ions, which reacted with CH_x derived from the CH_4 decomposition on the nickel surface to further improve the yield of syngas and carbon inhibition. As shown in Figure 6b, with the increase in Ce content, the carbon deposition decreased sharply, and the proportion of graphitized

carbon also reduced, suggesting an easier removal of coke. Quantitatively, when the Ce content was 15 wt.%, the carbon deposition was only 0.29 g/g_{cat}; moreover, the addition of Ce did not affect the conversion of CH₄ and CO₂, and maintained the dispersion and activity of Ni sites (Figure 6c) [89]. To further improve the oxygen mobility, ZrO₂ can be added to Ni/Ce–Al₂O₃. The formation of CeO₂/ZrO₂ solid solution generated more oxygen vacancies, increased the reducibility and enhanced the oxygen storage capacity, thus reducing the coke formation and improving the catalytic stability [90].

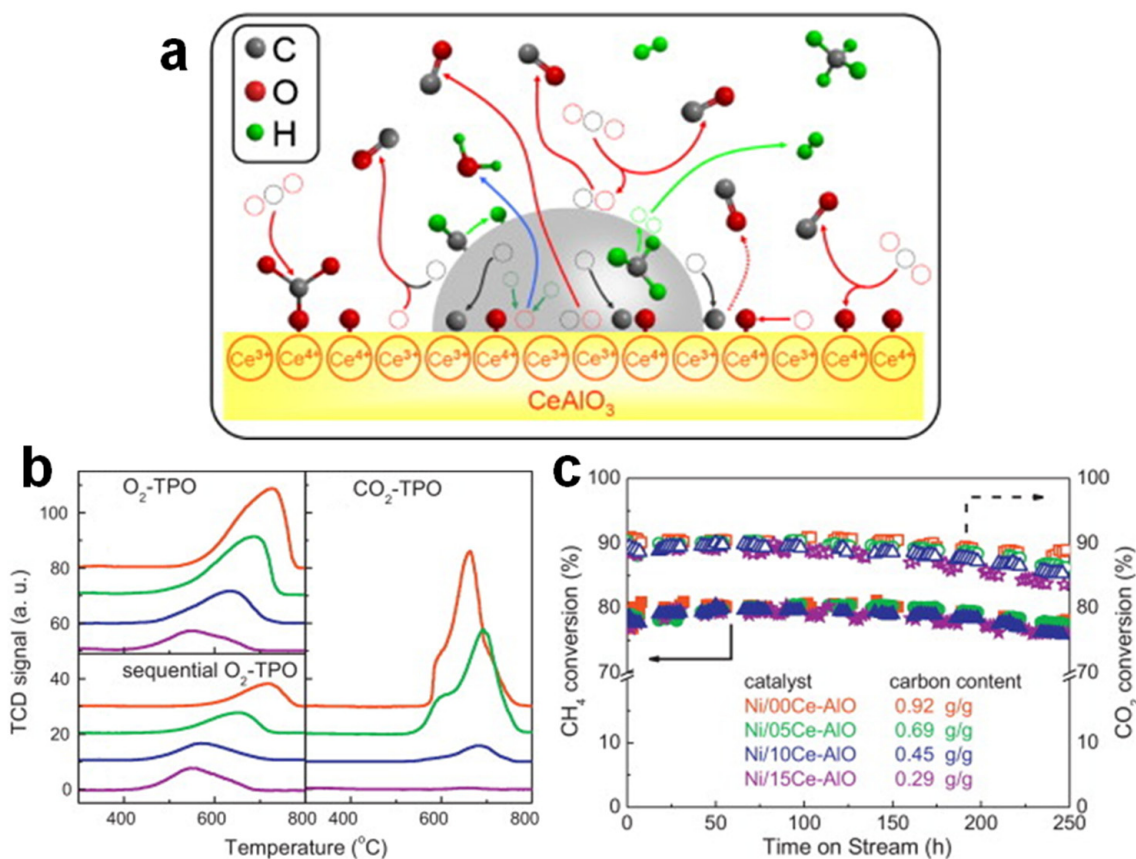


Figure 6. (a) Schematic representation of reaction and carbon deposition over Ni/Ce–AlO catalysts. (b) O₂-TPO, sequential CO₂-TPO and O₂-TPO profiles of the catalysts after 250 h DRM tests at 800 °C: Ni/00Ce–AlO (red), Ni/05Ce–AlO (green), Ni/10Ce–AlO (blue) and Ni/15Ce–AlO (purple). (c) Activity performance and carbon content of the catalysts in 250 h long-term tests. Reaction conditions: 800 °C, GHSV = 20,000 mL min^{−1} g^{−1}, atmospheric pressure. Square: Ni/00Ce–AlO; circle: Ni/05Ce–AlO; triangle: Ni/10Ce–AlO; star: Ni/15Ce–AlO. Reproduced with permission from [89]. Copyright 2013, Elsevier.

Other rare earth metals also exhibit excellent thermal stability, redox potential and good oxygen storage capacity. For example, Sm doping in Ni/Al₂O₃ lowers the reduction temperature and enhances the reducibility of Ni nanoparticles from Al₂O₃. Similarly to Ce, the redox property of Sm promotes oxygen transfer and CO₂ adsorption. In addition, the intrinsic high oxygen vacancy and the extra oxygen vacancies generated by the exchange of Ni²⁺ and Sm³⁺ ions facilitate the adsorption of CH₄, increasing the conversions and inhibiting coke formation in the DRM reaction [91]. Another rare earth metal oxide Y₂O₃, featuring excellent oxygen mobility and redox properties, can minimize the accumulation of different carbonaceous species on the spent catalyst surface by improving the coke gasification rate, leading to improved activity and stability [92]. In addition to Ce and Y, the addition of La₂O₃ to Ni/Al₂O₃ can control the decomposition of CH₄, the oxidation of carbon deposits by CO₂ and the inhibition of the graphitization of carbon deposits [40]. Figueredo et al. [93] prepared a Ni/La–Al₂O₃ catalyst and found that the addition of La

could stabilize the γ -Al₂O₃ structure and form perovskite LaAlO₃, possessing abundant oxygen vacancies and high structural stability. The oxygen vacancy in LaAlO₃ perovskite reduced the MSI and increased the metal active sites. Meanwhile, the high oxygen mobility of perovskite promoted the activation of C–H bonds, resulting in the catalytic activity of Ni for methane conversion [75,93].

Table 1. Summary of the Ni/Al₂O₃ catalysts in DRM reaction.

Catalyst	Preparation Method	Reaction Condition		CH ₄ Conversion	CO ₂ Conversion	Carbon Formation	Reference
		CO ₂ /CH ₄	Reaction Temperature				
FeNiAl catalyst	one-step EISA method	1	700 °C	72.5%	82.3%	3.8%	[72]
Ni _{0.05} Al ₁ O _{2-δ}	citric acid sol–gel method	1	650 °C	68.7%	80.4%	0.59 mg _C g _{cat} ^{−1} h ^{−1}	[17]
Ni/MgAl ₂ O ₄	wet impregnation	1	750 °C	96%	98%	8.95%	[83]
Ni/M–Al ₂ O ₃	incipient impregnation method	1	700 °C	77.6%	85.4%	3.5%	[26]
15%NiO/COMA	sequential impregnation	1	850 °C	98%	97%	1.3 g/ml	[1]
Ni/15%CeO ₂ –Al ₂ O ₃	incipient wetness impregnation	1	800 °C	80%	85%	0.29 g g _{cat} ^{−1}	[89]
Ni/La ₂ O ₃ –Al ₂ O ₃	stepwise incipient wetness impregnation.	1	650 °C	61%	65%	Less than 4%	[18]
Ni/Y–Al ₂ O ₃	co-precipitation	1	700 °C	74.4%	78.6%	Less than 12%	[47]
Ni supported on mesoporous alumina	incipient impregnation method	1	700 °C	77.6%	85.4%	3.8%	[27]
Ni/Al ₂ O ₃	solution combustion synthesis	1	800 °C	87%	94%	0.0378 g _C g _{cat} ^{−1} h ^{−1}	[80]
Ni–Co–Ru/MgO–Al ₂ O ₃	neutral sol–gel	1	800 °C	93.2%	92.5%	8.1 mg _C g _{cat} ^{−1} h ^{−1}	[65]
Ni _{0.8} Co _{0.2} Al ₂ O ₄	ultrasonic spray pyrolysis	1	750 °C	95%	95%	18.2%	[22]
10Ni–2Sn/Al ₂ O ₃	modified Pechini method	1	650 °C	33%	35%	7.2%	[73]

6. Conclusions and Prospects

In this review, several strategies of enhancing the coking and sintering resistance of Ni/Al₂O₃ in DRM reactions have been discussed in depth. Smart designs of hierarchical porous structures and 1D/2D nanomaterials can promote Ni dispersion and enlarge the surface area, thus preventing the metal agglomeration and increasing the number of active sites. Additionally, optimizing the surface acidity/basicity of alumina by adding alkali/alkaline metal oxides enables a better adsorption and activation of CO₂, promoting the syngas production and carbon removal. Moreover, the synergistic effects of Ni alloys and appropriate strength of the MSI hinder the migration of Ni and control the reducibility. Finally, the introduction of oxygen defects and generation of active surface oxygen species by adding rare earth metal oxides facilitate the oxygen movement and gasification of coke. Despite some progress made in related fields, there is still room for improvement, as discussed below.

Firstly, most of the modifications are limited to one or two functions. Certain improvements have to be at the expense of affecting other properties or performances. For example, the addition of Sn could slow down methane cracking and inhibit coke formation; however, coverage on the Ni active sites may reduce the conversions. In this situation, multi-functional catalysts are suggested to be developed to enhance the activity, stability and anti-deactivation properties simultaneously by taking advantages of the synergistic effects of each component in the catalyst. For instance, when mesoporous La₂O₃ is doped in Ni/Al₂O₃, the Ni dispersion, surface basicity, MSI and oxygen defects can be adjusted to a suitable level, achieving a robust and active catalyst.

Secondly, the specific role of the NiAl₂O₄ spinel phase is still in debate; either a promotional effect on the MSI or a negative impact on the metal active sites has been reported for DRM reactions. More systematic and mechanism studies are recommended to elucidate the exact formation process and the influences of the resultant spinel structure on the catalytic performance and deactivation behavior.

Thirdly, excessive basicity and MSI may not benefit the performance. Thus, investigations on the number of promoters (e.g., MgO) are recommended, as well as the thermal treatment parameters, in order to achieve a suitable degree of basicity and MSI for the optimized adsorption/activation of CO₂ molecules and generation of metal active sites for CH₄ dissociation.

Finally, understanding the deactivation mechanisms of Ni/Al₂O₃ lays the foundation for modifications of the development strategies. More efforts are expected to explore the coke generation and removal process and metal migration and agglomeration by taking advantage of advanced characterization techniques (e.g., in situ monitoring systems).

Author Contributions: Conceptualization, data curation, investigation, writing—original draft, X.G., Z.G., G.Z., and Z.W.; writing—review and editing; X.G. and Z.G.; project administration, supervision, validation J.A. and S.K.; funding acquisition, resources, S.K. All authors have read and agreed to the published version of the manuscript.

Funding: This research was funded by the Ministry of Education in Singapore (MOE) Tier 2 grant (WBS: R279-000-544-112), Singapore Agency for Science, Technology and Research (A*STAR) AME IRG grant (No. A1783c0016), Guangzhou Basic and Applied Basic Research Project in China (202102020134) and Youth Innovation Talents Project of Guangdong Universities (natural science) in China (2019KQNCX098).

Data Availability Statement: All data included in this study are available upon the permission from the publishers.

Conflicts of Interest: The authors declare no conflict of interest.

References

1. Gholizadeh, F.; Izadbakhsh, A.; Huang, J.; Yan, Z. Catalytic performance of cubic ordered mesoporous alumina supported nickel catalysts in dry reforming of methane. *Microporous Mesoporous Mater.* **2021**, *310*, 110616. [\[CrossRef\]](#)
2. Yusuf, M.; Farooqi, A.S.; Keong, L.K.; Hellgardt, K.; Abdullah, B. Contemporary trends in composite Ni-based catalysts for CO₂ reforming of methane. *Chem. Eng. Sci.* **2021**, *229*, 116072. [\[CrossRef\]](#)
3. Ranjekar, A.M.; Yadav, G.D. Dry reforming of methane for syngas production: A review and assessment of catalyst development and efficacy. *J. Indian Chem. Soc.* **2021**, *98*, 100002. [\[CrossRef\]](#)
4. Bu, K.K.; Deng, J.; Zhang, X.; Boon, S.C.K.; Yan, T.; Li, H.; Shi, L.; Zhang, D. Promotional effects of B-terminated defective edges of Ni/boron nitride catalysts for coking- and sintering-resistant dry reforming of methane. *Appl. Catal. B Environ.* **2020**, *267*, 118692. [\[CrossRef\]](#)
5. Yentekakis, I.V.; Panagiotopoulou, P.; Artemakis, G. A review of recent efforts to promote dry reforming of methane (DRM) to syngas production via bimetallic catalyst formulations. *Appl. Catal. B Environ.* **2021**, *296*, 120210. [\[CrossRef\]](#)
6. Li, B.; Yuan, X.; Li, B.; Wang, X. Impact of pore structure on hydroxyapatite supported nickel catalysts (Ni/HAP) for dry reforming of methane. *Fuel Process. Technol.* **2020**, *202*, 106359. [\[CrossRef\]](#)
7. Martin-del-Campo, J.; Uceda, M.; Coulombe, S.; Kopyscinski, J. Plasma-catalytic dry reforming of methane over Ni-supported catalysts in a rotating gliding arc-Spouted bed reactor. *J. CO₂ Util.* **2021**, *46*, 101474. [\[CrossRef\]](#)
8. Yang, B.; Deng, J.; Li, H.; Yan, T.; Zhang, J.; Zhang, D. Coking-resistant dry reforming of methane over Ni/ γ -Al₂O₃ catalysts by rationally steering metal-support interaction. *iScience* **2021**, *24*, 102747. [\[CrossRef\]](#)
9. Wang, Y.; Yao, L.; Wang, S.; Mao, D.; Hu, C. Low-temperature catalytic CO₂ dry reforming of methane on Ni-based catalysts: A review. *Fuel Process. Technol.* **2018**, *169*, 199–206. [\[CrossRef\]](#)
10. Zhang, G.; Liu, J.; Xu, Y.; Sun, Y. A review of CH₄-CO₂ reforming to synthesis gas over Ni-based catalysts in recent years (2010–2017). *Int. J. Hydrogen Energy* **2018**, *43*, 15030–15054. [\[CrossRef\]](#)
11. Sun, Y.; Zhang, G.; Xu, Y.; Zhang, Y.; Lv, Y.; Zhang, R. Comparative study on dry reforming of methane over Co-M (M = Ce, Fe, Zr) catalysts supported on N-doped activated carbon. *Fuel Process. Technol.* **2019**, *192*, 1–12. [\[CrossRef\]](#)
12. de Araújo Moreira, T.G.; de Carvalho Filho, J.F.S.; Carvalho, Y.; de Almeida, J.M.A.R.; Romano, P.N.; Sousa-Aguiar, E.F. Highly stable low noble metal content rhodium-based catalyst for the dry reforming of methane. *Fuel* **2021**, *287*, 119536. [\[CrossRef\]](#)
13. Horlyck, J.; Lawrey, C.; Lovell, E.C.; Amal, R.; Scott, J. Elucidating the impact of Ni and Co loading on the selectivity of bimetallic NiCo catalysts for dry reforming of methane. *Chem. Eng. J.* **2018**, *352*, 572–580. [\[CrossRef\]](#)
14. Xu, Y.; Du, X.; Shi, L.; Chen, T.; Wan, H.; Wang, P.; Wei, S.; Yao, B.; Zhu, J.; Song, M. Improved performance of Ni/Al₂O₃ catalyst deriving from the hydrotalcite precursor synthesized on Al₂O₃ support for dry reforming of methane. *Int. J. Hydrogen Energy* **2021**, *46*, 14301–14310. [\[CrossRef\]](#)
15. Park, K.S.; Cho, J.M.; Park, Y.M.; Kwon, J.H.; Yu, J.; Jeong, H.E.; Choung, J.W.; Bae, J.W. Enhanced thermal stability of Ni nanoparticles in ordered mesoporous supports for dry reforming of methane with CO₂. *Catal. Today* **2020**. [\[CrossRef\]](#)
16. Xu, Y.; Du, X.; Li, J.; Wang, P.; Zhu, J.; Ge, F.; Zhou, J.; Song, M.; Zhu, W. A comparison of Al₂O₃ and SiO₂ supported Ni-based catalysts in their performance for the dry reforming of methane. *J. Fuel Chem. Technol.* **2019**, *47*, 199–208. [\[CrossRef\]](#)
17. Zhang, S.; Ying, M.; Yu, J.; Zhan, W.; Wang, L.; Guo, Y.; Guo, Y. Ni_xAl₁O_{2- δ} mesoporous catalysts for dry reforming of methane: The special role of NiAl₂O₄ spinel phase and its reaction mechanism. *Appl. Catal. B Environ.* **2021**, *291*, 120074. [\[CrossRef\]](#)
18. Li, K.; Pei, C.; Li, X.; Chen, S.; Zhang, X.; Liu, R.; Gong, J. Dry reforming of methane over La₂O₂CO₃-modified Ni/Al₂O₃ catalysts with moderate metal support interaction. *Appl. Catal. B Environ.* **2020**, *264*, 118448. [\[CrossRef\]](#)

19. Ma, Q.; Han, Y.; Wei, Q.; Makpal, S.; Gao, X.; Zhang, J.; Zhao, T. Stabilizing Ni on bimodal mesoporous-macroporous alumina with enhanced coke tolerance in dry reforming of methane to syngas. *J. CO₂ Util.* **2020**, *35*, 288–297. [[CrossRef](#)]
20. Li, Z.; Lin, Q.; Li, M.; Cao, J.; Liu, F.; Pan, H.; Wang, Z.; Kawi, S. Recent advances in process and catalyst for CO₂ reforming of methane. *Renew. Sust. Energ. Rev.* **2020**, *134*, 110312. [[CrossRef](#)]
21. Zhang, L.; Wang, X.; Shang, X.; Tan, M.; Ding, W.; Lu, X. Carbon dioxide reforming of methane over mesoporous nickel aluminate/ γ -alumina composites. *J. Energy Chem.* **2017**, *26*, 93–100. [[CrossRef](#)]
22. Aghaali, M.H.; Firoozi, S. Enhancing the catalytic performance of Co substituted NiAl₂O₄ spinel by ultrasonic spray pyrolysis method for steam and dry reforming of Methane. *Int. J. Hydrogen Energy* **2021**, *46*, 357–373. [[CrossRef](#)]
23. Marinho, A.L.A.; Toniolo, F.S.; Noronha, F.B.; Epron, F.; Bion, D.D.N. Highly active and stable Ni dispersed on mesoporous CeO₂-Al₂O₃ catalysts for production of syngas by dry reforming of methane. *Appl. Catal. B Environ.* **2021**, *281*, 119459. [[CrossRef](#)]
24. Wei, Q.; Gao, X.; Liu, G.; Yang, R.; Zhang, H.; Yang, G.; Yoneyama, Y.; Tsubaki, N. Facile one-step synthesis of mesoporous Ni-Mg-Al catalyst for syngas production using coupled methane reforming process. *Fuel* **2018**, *211*, 1–10. [[CrossRef](#)]
25. Zhou, X.; Song, K.; Li, Z.; Kang, W.; Ren, H.; Su, K.; Zhang, M.; Cheng, B. The excellent catalyst support of Al₂O₃ fibers with needle-like mullite structure and HMF oxidation into FDCA over CuO/Al₂O₃ fibers. *Ceram. Int.* **2019**, *45*, 2330–2337. [[CrossRef](#)]
26. Jabbour, K.; Saad, A.; Inaty, L.; Davidson, A.; Massiani, P.; Hassan, N.E. Ordered mesoporous Fe-Al₂O₃ based-catalysts synthesized via a direct “one-pot” method for the dry reforming of a model biogas mixture. *Int. J. Hydrogen Energy* **2019**, *144*, 14889–14907. [[CrossRef](#)]
27. Bian, Z.; Zhong, W.; Yu, Y.; Wang, Z.; Jiang, B.; Kawi, S. Dry reforming of methane on Ni/mesoporous-Al₂O₃ catalysts: Effect of calcination temperature. *Int. J. Hydrogen Energy* **2021**, *46*, 31041–31053. [[CrossRef](#)]
28. Barelli, L.; Bidini, G.; Di Michele, A.; Gammaitoni, L.; Mattarelli, M.; Mondì, F.; Sisani, E. Development and validation of a Ni-based catalyst for carbon dioxide dry reforming of methane process coupled to solid oxide fuel cells. *Int. J. Hydrogen Energy* **2019**, *44*, 16582–16593. [[CrossRef](#)]
29. Lyu, L.; Han, Y.; Ma, Q.; Makpal, S.; Sun, J.; Gao, X.; Zhang, J.; Fan, H.; Zhao, T.-S. Fabrication of Ni-Based Bimodal Porous Catalyst for Dry Reforming of Methane. *Catalysts* **2020**, *10*, 1220. [[CrossRef](#)]
30. Bao, Z.; Lu, Y.; Han, J.; Li, Y.; Yu, F. Highly Active and Stable Ni-based Bimodal Pore Catalyst for Dry Reforming of Methane. *Appl. Catal. A Gen.* **2015**, *491*, 116–126. [[CrossRef](#)]
31. Gonzalez, J.J.; Da Costa-Serra, J.F.; Chica, A. Biogas dry reforming over Ni-Ce catalyst supported on nanofibered alumina. *Int. J. Hydrogen Energy* **2020**, *45*, 20568–20581. [[CrossRef](#)]
32. Hambali, H.U.; Jalil, A.A.; Abdurashed, A.A.; Siang, T.J.; Vo, D.V.N. Enhanced dry reforming of methane over mesostructured fibrous Ni/MFI zeolite: Influence of preparation methods. *J. Energy Inst.* **2020**, *93*, 1535–1543. [[CrossRef](#)]
33. Liang, T.Y.; Chen, H.H.; Tsai, D.H. Nickel hybrid nanoparticle decorating on alumina nanoparticle cluster for synergistic catalysis of methane dry reforming. *Fuel Process. Technol.* **2020**, *201*, 106335. [[CrossRef](#)]
34. Sun, J.W.; Wang, S.; Guo, Y.; Li, M.; Zou, H.; Wang, Z. Carbon dioxide reforming of methane over nanostructured Ni/Al₂O₃ catalysts. *Catal. Commun.* **2018**, *104*, 53–56. [[CrossRef](#)]
35. Jawad, A.; Rezaei, F.; Rownaghi, A.A. Highly Efficient Pt/Mo-Fe/Ni-Based Al₂O₃-CeO₂ Catalysts for Dry Reforming of Methane. *Catal. Today* **2019**, *350*, 80–90. [[CrossRef](#)]
36. Tsipourari, V.A.; Verykios, X.E. Kinetic study of the catalytic reforming of methane with carbon dioxide to synthesis gas over Ni/La₂O₃ catalyst. *Catal. Today* **2001**, *64*, 83–90. [[CrossRef](#)]
37. Gao, X.; Ashok, J.; Kawi, S. A review on roles of pretreatment atmospheres for the preparation of efficient Ni-based catalysts. *Catal. Today* **2021**. [[CrossRef](#)]
38. Menegazzo, F.; Pizzolitto, C.; Ghedini, E.; Di Michele, A.; Cruciani, G.; Signoretto, M. Development of La Doped Ni/CeO₂ for CH₄/CO₂ Reforming. *C J. Carbon Res.* **2018**, *4*, 60. [[CrossRef](#)]
39. Ni, J.; Zhao, J.; Chen, L.; Lin, J.; Kawi, S. Lewis acid sites stabilized nickel catalysts for dry (CO₂) reforming of methane. *ChemCatChem* **2016**, *8*, 3732–3739. [[CrossRef](#)]
40. Al-Mubaddel, F.S.; Kumar, R.; Sofiu, M.L.; Frusteri, F.; Ibrahim, A.A.; Srivastava, V.K.; Kasim, S.O.; Fakeeha, A.H.; Abasaheed, A.E.; Osman, A.I.; et al. Optimizing acido-basic profile of support in Ni supported La₂O₃ + Al₂O₃ catalyst for dry reforming of methane. *Int. J. Hydrogen Energy* **2021**, *46*, 14225–14235. [[CrossRef](#)]
41. Al-Fatesh, A.S.; Naeem, M.A.; Fakeeha, A.H.; Abasaheed, A.E. Role of La₂O₃ as Promoter and Support in Ni/ γ -Al₂O₃ Catalysts for Dry Reforming of Methane. *Chin. J. Chem. Eng.* **2014**, *22*, 28–37. [[CrossRef](#)]
42. Khoja, A.H.; Tahir, M.; Amin, N.A.S. Evaluating the performance of Ni catalyst supported on La₂O₃-MgAl₂O₄ for dry reforming of methane in a packed bed dielectric barrier discharge (DBD) plasma reactor. *Energy Fuels* **2019**, *33*, 11630–11647. [[CrossRef](#)]
43. Alipour, Z.; Rezaei, M.; Meshkani, F. Effect of alkaline earth promoters (MgO, CaO, and BaO) on the activity and coke formation of Ni catalysts supported on nanocrystalline Al₂O₃ in dry reforming of methane. *J. Ind. Eng. Chem.* **2014**, *20*, 2858–2863. [[CrossRef](#)]
44. Khoja, A.H.; Tahir, M.; Amin, N.A.S. Cold plasma dielectric barrier discharge reactor for dry reforming of methane over Ni/ γ -Al₂O₃-MgO nanocomposite. *Fuel Process. Technol.* **2018**, *178*, 166–179. [[CrossRef](#)]
45. Cho, E.; Lee, Y.-H.; Kim, H.; Jang, E.J.; Kwak, J.H.; Lee, K.; Ko, C.H.; Yoon, W.L. Ni Catalysts for Dry Methane Reforming Prepared by A-site Exsolution on Mesoporous Defect Spinel Magnesium Aluminate. *Appl. Catal. A Gen.* **2020**, *602*, 117694. [[CrossRef](#)]
46. Gao, X.; Ashok, J.; Kawi, S. Smart Designs of Anti-Coking and Anti-Sintering Ni-Based Catalysts for Dry Reforming of Methane: A Recent Review. *Reactions* **2020**, *1*, 162–194. [[CrossRef](#)]

47. Świrk, K.; Gálvez, M.E.; Motak, M.; Grzybek, T.; Rønning, M.; Da Costa, P. Yttrium promoted Ni-based double-layered hydroxides for dry methane Reforming. *J. CO₂ Util.* **2018**, *27*, 247–258. [[CrossRef](#)]
48. Bang, S.; Hong, E.; Baek, S.W.; Shin, C.-H. Effect of Acidity on Ni Catalysts Supported on P-modified Al₂O₃ for Dry Reforming of Methane. *Catal. Today* **2018**, *303*, 100–105. [[CrossRef](#)]
49. Yang, E.-H.; Moon, D.J. CO₂ Reforming of Methane over Ni⁰/La₂O₃ Catalyst Without Reduction Step: Effect of Calcination Atmosphere. *Top. Catal.* **2017**, *60*, 697–705. [[CrossRef](#)]
50. Bai, J.; Liu, K.; Xie, S.; Xu, L.; Lin, L. Effect of Mg addition on catalytic performance of Mo/ZSM-5 catalyst for methane aromatization. *Chin. J. Catal.* **2004**, *25*, 70–74.
51. Wang, H.; Chen, S.; Yuan, G.; Wang, Z.; Cai, Z. Effects of N₂ Pretreatment on Acidity and Catalytic Performance of Re₂O₇/Al₂O₃. *Chem. Eng. Oil Gas.* **2010**, *4*, 277–280.
52. Santamaria, L.; Lopez, G.; Fernandez, E.; Cortazar, M.; Arregi, A.; Olazar, M.; Bilbao, J. Progress on Catalyst Development for the Steam Reforming of Biomass and Waste Plastics Pyrolysis Volatiles: A Review. *Energy Fuels* **2021**. [[CrossRef](#)]
53. Egelske, B.T.; Keels, J.M.; Monnier, J.R.; Regalbuto, J.R. An analysis of electroless deposition derived Ni-Pt catalysts for the dry reforming of methane. *J. Catal.* **2020**, *381*, 374–384. [[CrossRef](#)]
54. Tomishige, K.; Kanazawa, S.; Ito, S.I.; Kunimori, K. Catalyst development for direct heat supply from combustion to reforming in methane reforming with CO₂ and O₂. *Appl. Catal. A Gen.* **2003**, *244*, 71–82. [[CrossRef](#)]
55. Ozkara-Aydinoglu, S.; Aksoylu, A.E. CO₂ reforming of methane over Pt-Ni/Al₂O₃ catalysts: Effects of catalyst composition, and water and oxygen addition to the feed. *Int. J. Hydrogen Energy* **2011**, *36*, 2950–2959. [[CrossRef](#)]
56. García-Diéguez, M.; Pieta, I.S.; Herrera, M.C.; Larrubia, M.A.; Alemany, L.J. Nanostructured Pt- and Ni-based catalysts for CO₂-reforming of methane. *J. Catal.* **2010**, *270*, 136–145. [[CrossRef](#)]
57. Mahoney, E.G.; Pusel, J.M.; Stagg-Williams, S.M.; Faraji, S. The effects of Pt addition to supported Ni catalysts on dry (CO₂) reforming of methane to syngas. *J. CO₂ Util.* **2014**, *6*, 40–44. [[CrossRef](#)]
58. De, S.; Zhang, J.; Luque, R.; Yan, N. Ni-based bimetallic heterogeneous catalysts for energy and environmental applications. *Energy Environ. Sci.* **2016**, *9*, 3314–3347. [[CrossRef](#)]
59. Theofanidis, S.-A.; Pieterse, J.A.Z.; Poelman, H.; Longo, A.; Sabbe, M.K.; Virginie, M.; Detavernier, C.; Marin, G.B.; Galvita, V.V. Effect of Rh in Ni-based catalysts on sulfur impurities during methane reforming. *Appl. Catal. B Environ.* **2020**, *267*, 118691. [[CrossRef](#)]
60. Bian, Z.; Das, S.; Wai, M.H.; Hongmanorom, P.; Kawi, S. A Review on Bimetallic Nickel-Based Catalysts for CO₂ Reforming of Methane. *ChemPhysChem* **2017**, *18*, 3117–3134. [[CrossRef](#)] [[PubMed](#)]
61. Ocsachoque, M.A.; Aparicio, M.S.L.; Gonzalez, M.G. Effect of Rh Addition to Ni/MgO-Al₂O₃ Catalysts for Dry Reforming of Methane. *Indian J. Sci. Technol.* **2017**, *10*, 1–9. [[CrossRef](#)]
62. Damyanova, S.; Shtereva, I.; Pawelec, B.; Mihaylov, L.; Fierro, J.L.G. Characterization of none and yttrium-modified Ni-based catalysts for dry reforming of methane. *Appl. Catal. B Environ.* **2020**, *278*, 119335. [[CrossRef](#)]
63. Liu, A.; Praserthdam, S.; Phatanasri, S. Investigation on the increased stability of the Ni-Co bi-metallic catalysts for the carbon dioxide reforming of methane. *Catal. Today* **2020**, *358*, 37–44. [[CrossRef](#)]
64. Joo, S.; Seong, A.; Kwon, O.; Kim, K.; Lee, J.H.; Gorte, R.J.; Vohs, J.M.; Han, J.W.; Kim, G. Highly active dry methane reforming catalysts with boosted in situ grown Ni-Fe nanoparticles on perovskite via atomic layer deposition. *Sci. Adv.* **2020**, *6*, eabb1573. [[CrossRef](#)] [[PubMed](#)]
65. Aramouni, N.A.K.; Zeaiter, J.; Kwapinski, W.; Leahy, J.J.; Ahmad, M.N. Eclectic trimetallic Ni-Co-Ru catalyst for the dry reforming of methane. *Int. J. Hydrogen Energy* **2020**, *45*, 17153–17163. [[CrossRef](#)]
66. Chatla, A.; Ghouri, M.M.; Hassan, O.W.E.; Mohamed, N.; Prakash, A.V.; Elbasher, N.O. An experimental and first principles DFT investigation on the effect of Cu addition to Ni/Al₂O₃ catalyst for the dry reforming of methane. *Appl. Catal. A Gen.* **2020**, *602*, 117699. [[CrossRef](#)]
67. Nataj, S.M.M.; Alavi, S.M.; Mazloom, G. Modeling and optimization of methane dry reforming over Ni-Cu/Al₂O₃ catalyst using Box-Behnken design. *J. Energy Chem.* **2018**, *27*, 1475–1488. [[CrossRef](#)]
68. Wu, T.; Zhang, Q.; Cai, W.; Zhang, P.; Song, X.; Sun, Z.; Gao, L. Phyllosilicate evolved hierarchical Ni- and Cu-Ni/SiO₂ nanocomposites for methane dry reforming catalysis. *Appl. Catal. A Gen.* **2015**, *503*, 94–102. [[CrossRef](#)]
69. Rahemi, N.; Haghghi, M.; Babaluo, A.A.; Jafari, M.F.; Khorram, S. Non-thermal plasma assisted synthesis and physicochemical characterizations of Co and Cu doped Ni/Al₂O₃ nanocatalysts used for dry reforming of methane. *Int. J. Hydrogen Energy* **2013**, *38*, 16048–16061. [[CrossRef](#)]
70. Kim, S.M.; Abdala, P.M.; Margossian, T.; Hosseini, D.; Foppa, L.; Armutlulu, A.; van Beek, W.; Comas-Vives, A.; Copéret, C.; Müller, C. Cooperativity and Dynamics Increase the Performance of NiFe Dry Reforming Catalysts. *J. Am. Chem. Soc.* **2017**, *139*, 1937–1949. [[CrossRef](#)]
71. Ray, K.; Sengupta, S.; Deo, G. Reforming and cracking of CH₄ over Al₂O₃ supported Ni, Ni-Fe and Ni-Co catalysts. *Fuel Process. Technol.* **2017**, *156*, 195–203. [[CrossRef](#)]
72. Li, B.; Luo, Y.; Li, B.; Yuan, X.; Wang, X. Catalytic performance of iron-promoted nickel-based ordered mesoporous alumina FeNiAl catalysts in dry reforming of methane. *Fuel Process. Technol.* **2019**, *193*, 348–360. [[CrossRef](#)]
73. de Assis Rocha da Silva, F.; dos Santos, R.C.R.; Nunes, R.S.; Valentini, A. Role of tin on the electronic properties of Ni/Al₂O₃ catalyst and its effect over the methane dry reforming reaction. *Appl. Catal. A Gen.* **2021**, *618*, 118129. [[CrossRef](#)]

74. Guharoy, U.; Le Saché, E.; Cai, Q.; Reina, T.R.; Gu, S. Understanding the role of Ni-Sn interaction to design highly effective CO₂ conversion catalysts for dry reforming of methane. *J. CO₂ Util.* **2018**, *27*, 1–10. [[CrossRef](#)]
75. Stroud, T.; Smith, T.; Le Saché, E.; Santos, J.L.; Centeno, M.A.; Arellano-Garcia, H.; Odriozola, J.A.; Reina, T.R. Chemical CO₂ recycling via dry and bi reforming of methane using Ni-Sn/Al₂O₃ and Ni-Sn/CeO₂-Al₂O₃ catalysts. *Appl. Catal. B Environ.* **2018**, *224*, 125–135. [[CrossRef](#)]
76. Zhou, L.; Li, L.; Wei, N.; Li, J.; Basset, J.-M. Effect of NiAl₂O₄ Formation on Ni/Al₂O₃ Stability during Dry Reforming of Methane. *ChemCatChem* **2015**, *7*, 2508–2516. [[CrossRef](#)]
77. Wang, F.; Xu, L.; Zhang, J.; Zhao, Y.; Li, H.; Li, H.; Wu, K.; Xu, G.; Chen, W. Tuning the metal-support interaction in catalysts for highly efficient methane dry reforming reaction. *Appl. Catal. B Environ.* **2016**, *180*, 511–520. [[CrossRef](#)]
78. Adamu, S.; Bawah, A.-R.; Murazaa, O.; Malaibaria, Z.; Hossain, M.M. Effects of metal support interaction on dry reforming of methane over Ni/Ce-Al₂O₃ Catalysts. *Can. J. Chem. Eng.* **2020**, *98*, 2425–2434. [[CrossRef](#)]
79. Mette, K.; Kuhl, S.; Tarasov, A.; Willinger, M.G.; Krohnert, J.; Wrabetz, S.; Trunschke, A.; Scherzer, M.; Girgsdies, F.; Dudder, H.; et al. High-Temperature Stable Ni Nanoparticles for the Dry Reforming of Methane. *ACS Catal.* **2016**, *6*, 7238–7248. [[CrossRef](#)]
80. Ali, S.; Khader, M.M.; Almarri, M.J.; Abdelmoneim, A.G. Ni-based Nano-catalysts for the Dry Reforming of Methane. *Catal. Today* **2020**, *343*, 26–37. [[CrossRef](#)]
81. Dias, J.A.C.; Assaf, J.M. Influence of calcium content in Ni/CaO/γ-Al₂O₃ catalysts for CO₂-reforming of methane. *Catal. Today* **2003**, *85*, 59–68. [[CrossRef](#)]
82. Kim, M.-J.; Youn, J.-R.; Kim, H.J.; Seo, M.W.; Lee, D.; Go, K.S.; Lee, K.B.; Jeon, S.G. Effect of surface properties controlled by Ce addition on CO₂ methanation over Ni/Ce/Al₂O₃ Catalyst. *Int. J. Hydrogen Energy* **2020**, *45*, 24595–24603. [[CrossRef](#)]
83. Akiki, E.; Akiki, D.; Italiano, C.; Vita, A.; Abbas-Ghaleb, R.; Chlala, D.; Ferrante, G.D.; Lagana, M.; Pino, L.; Specchia, S. Production of hydrogen by methane dry reforming: A study on the effect of cerium and lanthanum on Ni/MgAl₂O₄ catalyst performance. *Int. J. Hydrogen Energy* **2020**, *45*, 21392–21408. [[CrossRef](#)]
84. Tu, P.H.; Le, D.N.; Dao, T.D.; Tran, Q.-T.; Doan, T.C.D.; Shiratori, Y.; Dang, C.M. Paper-structured catalyst containing CeO₂-Ni flowers for dry reforming of methane. *Int. J. Hydrogen Energy* **2020**, *45*, 18363–18375. [[CrossRef](#)]
85. Price, C.A.H.; Arnold, W.; Pastor-Pérez, L.; Amini-Horri, B.; Reina, T.R. Catalytic Upgrading of a Biogas Model Mixture via Low Temperature DRM Using Multicomponent Catalysts. *Top. Catal.* **2020**, *63*, 281–293. [[CrossRef](#)]
86. Kawi, S.; Kathiraser, Y.; Ni, J.; Oemar, U.; Li, Z.; Saw, E.T. Progress in Synthesis of Highly Active and Stable Nickel-Based Catalysts for Carbon Dioxide Reforming of Methane. *ChemSusChem* **2015**, *8*, 3556–3575. [[CrossRef](#)] [[PubMed](#)]
87. Horváth, A.; Németh, M.; Beck, A.; Maróti, B.; Sáfrán, G.; Pantaleo, G.; Liotta, L.F.; Venezia, A.M.; La Parola, V. Strong impact of indium promoter on Ni/Al₂O₃ and Ni/CeO₂-Al₂O₃ catalysts used in dry reforming of methane. *Appl. Catal. A Gen.* **2021**, *621*, 118174. [[CrossRef](#)]
88. Xu, G.; Shi, K.; Gao, Y.; Xu, H.; Wei, Y. Studies of reforming natural gas with carbon dioxide to produce synthesis gas: X. The role of CeO₂ and MgO promoters. *J. Mol. Catal. A Chem.* **1999**, *147*, 47–54. [[CrossRef](#)]
89. Chen, W.; Zhao, G.; Xue, Q.; Chen, L.; Lu, Y. High carbon-resistance Ni/CeAlO₃-Al₂O₃ catalyst for CH₄/CO₂ reforming. *Appl. Catal. B Environ.* **2013**, *136–137*, 260–268. [[CrossRef](#)]
90. Faria, E.C.; Neto, R.C.R.; Colman, R.C.; Noronha, F.B. Hydrogen production through CO₂ reforming of methane over Ni/CeZrO₂/Al₂O₃ catalysts. *Catal. Today* **2014**, *228*, 138–144. [[CrossRef](#)]
91. Taherian, Z.; Gharahshiran, V.S.; Fazlikhani, F.; Yousefpour, M. Catalytic performance of Samarium-modified Ni catalysts over Al₂O₃-CaO support for dry reforming of methane. *Int. J. Hydrogen Energy* **2020**, *46*, 7254–7262. [[CrossRef](#)]
92. Bahari, M.B.; Setiabudi, H.D.; Nishino, T.; Ayas, N.; Vo, D.V.N. Coke-resistant Y₂O₃-promoted cobalt supported on mesoporous alumina for enhanced hydrogen production. *J. Energy Inst.* **2021**, *94*, 272–284. [[CrossRef](#)]
93. Figueredo, G.P.; Medeiros, R.L.B.A.; Macedo, H.P.; de Oliveira, A.A.S.; Braga, R.M.; Mercury, J.M.R.; Melo, M.A.F.; Melo, D.M.A. A comparative study of dry reforming of methane over nickel catalysts supported on perovskite-type LaAlO₃ and commercial α-Al₂O₃. *Int. J. Hydrogen Energy* **2018**, *43*, 11022–11037. [[CrossRef](#)]